COMSOL Conference 2015 Boston

Session: Computational Fluid Dynamics

Boston Marriot Newton   Charles River West
Boston, MA   1:00 pm-2:45 pm
October 8th, 2015.

Fluid Motion Between Rotating Concentric Cylinders Using COMSOL Multiphysics™

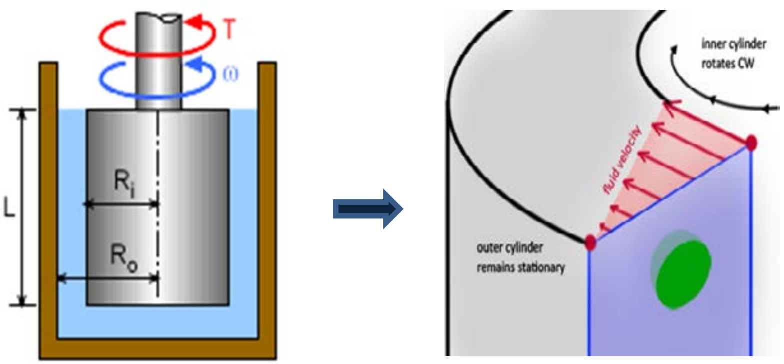

Kabita Barman
Sravanthi Mothupally
Archana Sonejee
Patrick L.Mills*

Department of Chemical and Natural Gas Engineering
Texas A & M University-Kingsville
Kingsville-TX 78363-8202 USA
*Patrick.Mills@tamuk.edu

TEXAS A&M UNIVERSITY KINGSVILLE

COMSOL CONFERENCE 2015 BOSTON

Outline

- Introduction
- Historical Background
- Applications
- Governing Equations
- Results and Discussion
- Computational Challenges
- Key Observations

Couette Viscometer

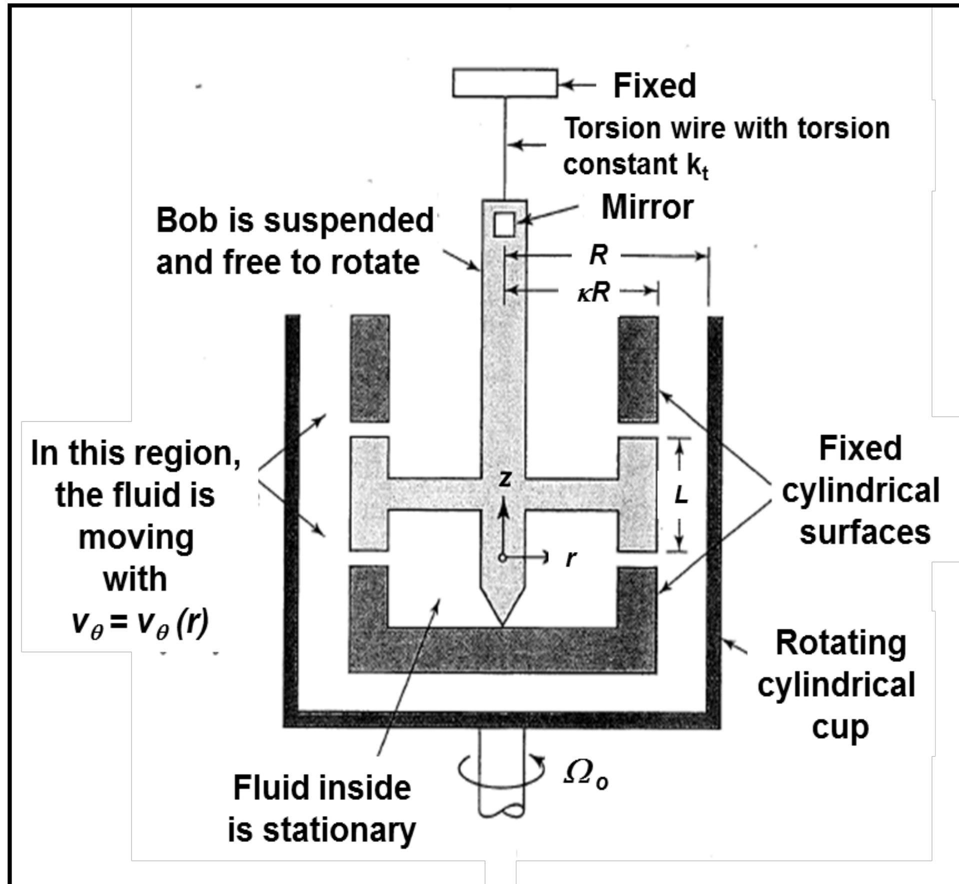

Introduction

- Fluid flow patterns contained between two concentric rotating cylinders has received noticeable attention in various fields of study.

- One widely used application of this system is the *rotational viscometer*. This study focuses on the analysis of CFD of a Newtonian incompressible fluid in the annular gap for the case where non-ideal end effects are included using COMSOL Multiphysics ™.

- The torque behavior imparted by fluid on the inner cylinder is evaluated to better understand non ideal fluid behavior.

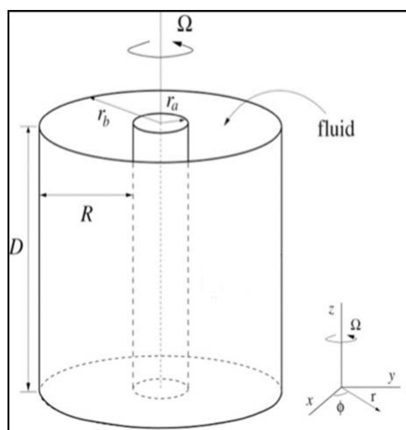

Monitoring and Control Laboratories

Historical Background

- The study of flow behavior of fluid comprised between two cylinder has a rich experimental history.
- Sir George Gabriel Stokes first mentioned it in the *Transactions of the Cambridge Philosophical Society* in 1848.
- Max Margules was the first to propose constructing a viscometer based on the rotating cylinder principle in 1881.
- In 1888, Arnulph Mallock did an experiment on the viscosity of water using a pair of concentric cylinders.
- In 1890, Couette published a study of viscosity using a pair of cylinders where the outer one was rotating and inner one suspended on a fiber.

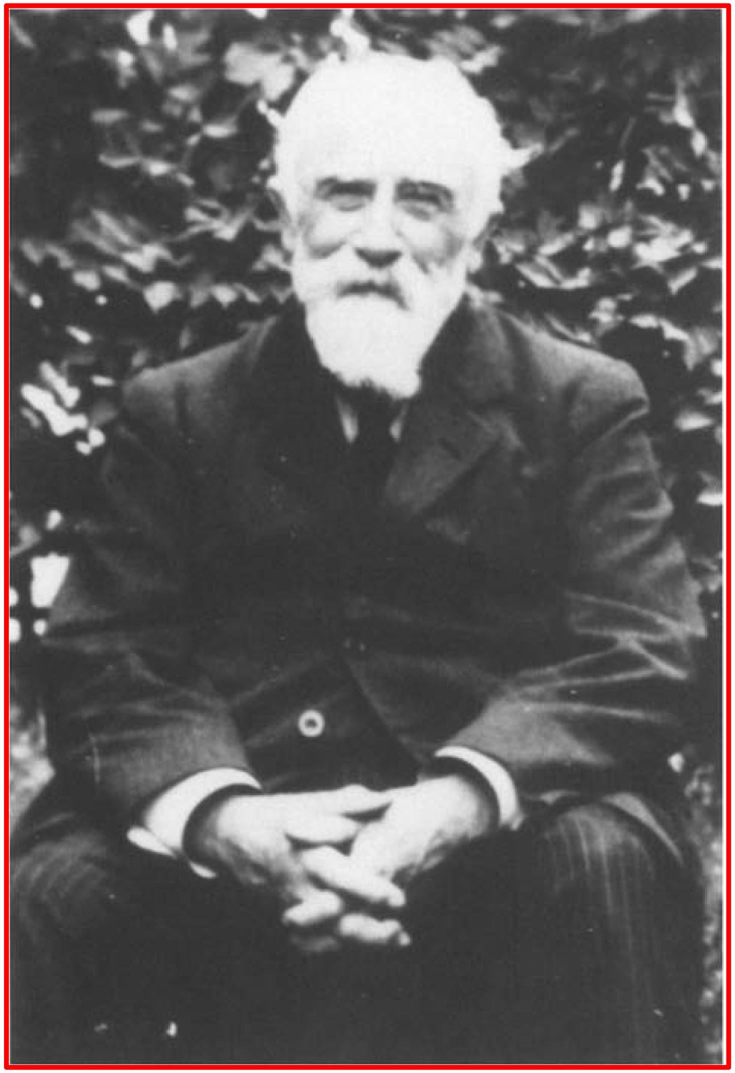

Maurice Couette (1858 – 1953)
Rheologica Acta 33:357-368 (1994)

Early Viscometer Designs

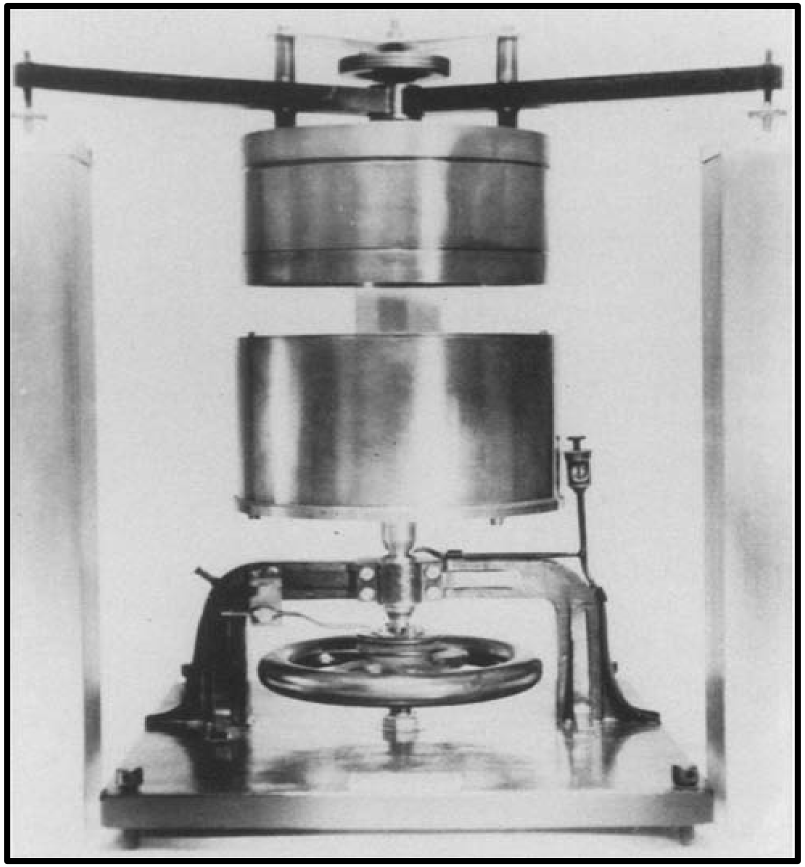

The cylinder viscometer of M. Couette (1888)
(Rheologica Acta 33:357-368 (1994))

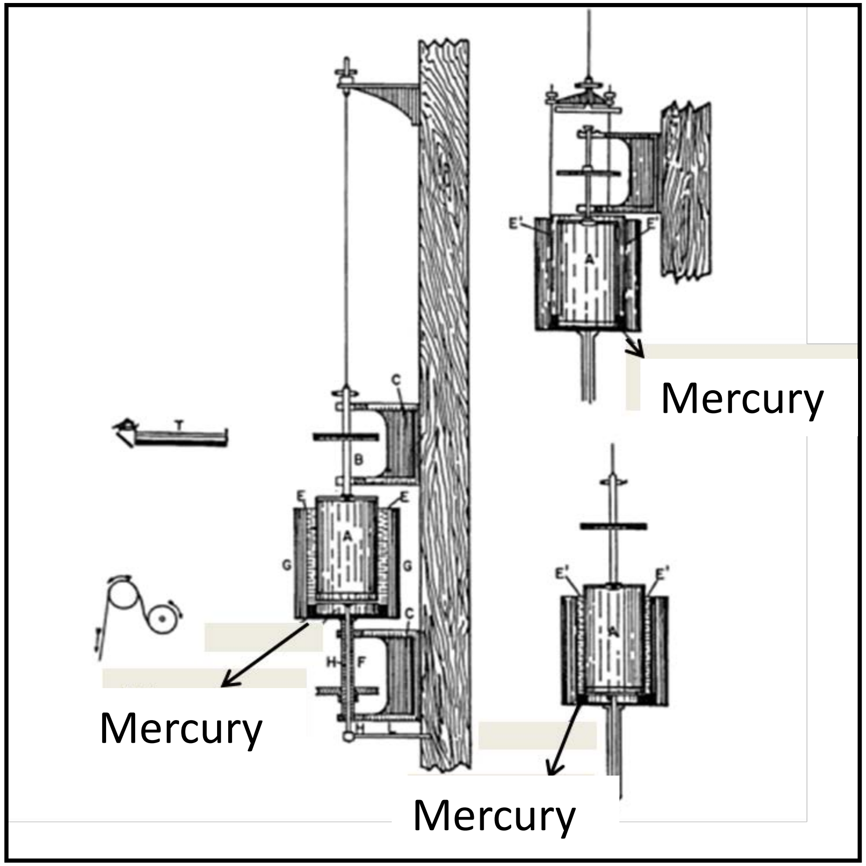

Arnulph Mallock's apparatus (1888)*

From 18th century to now, many developments in this field have occurred and are still ongoing .

***Reference**: C. David Andereck andF. Hayot, "Ordered and Turbulent Patterns in Taylor-Couette Flow", The Ohio State University, Columbus, Ohio, NATO ASI Series, Series B: Physics Vol.297

Industrial Applications of Annular Flows

- Production of oil and gas
- Centrifugally-driven separation processes
- Electrochemical cells
- Viscometers
- Tribology
- Hydraulic equipment
- Chemical reactors

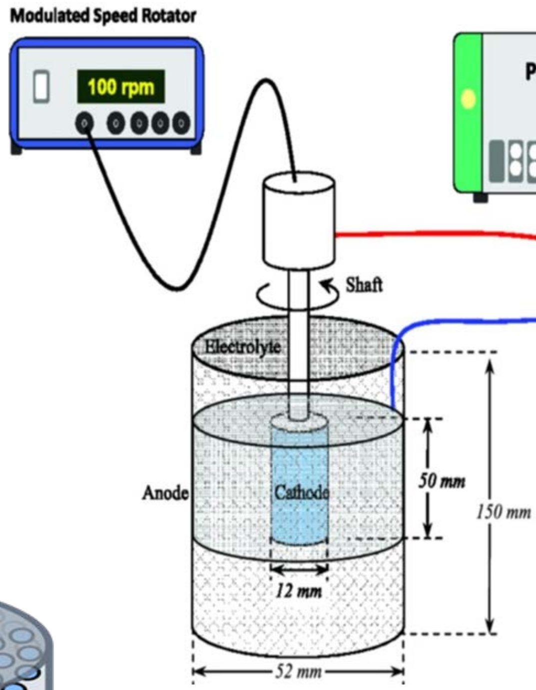

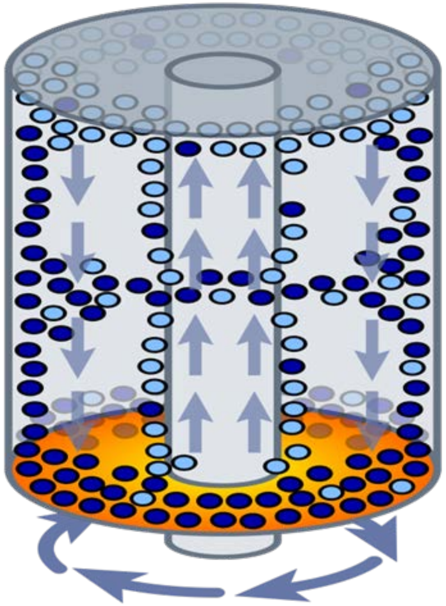

Navier-Stokes Equations in Polar Coordinates

Polar Component Form

r – component

$$\rho\left(\frac{\partial v_r}{\partial t}+v_r\left(\frac{\partial v_r}{\partial r}\right)+\frac{v_\theta}{r}\left(\frac{\partial v_r}{\partial \theta}\right)+v_z\left(\frac{\partial v_r}{\partial z}\right)-\frac{v_\theta^2}{r}\right)$$
$$=-\left(\frac{\partial p(r,z)}{\partial r}\right)+\rho g_r+\mu\left(\frac{\partial}{\partial r}\left(\frac{1}{r}\frac{\partial(r v_r)}{\partial r}\right)+\frac{1}{r^2}\frac{\partial^2 v_r}{\partial \theta^2}+\frac{\partial^2 v_r}{\partial z^2}-\frac{2}{r^2}\left(\frac{\partial v_\theta}{\partial \theta}\right)\right)$$

θ – component

$$\rho\left(\frac{\partial v_\theta}{\partial t}+v_r\left(\frac{\partial v_\theta}{\partial r}\right)+\frac{v_\theta}{r}\left(\frac{\partial v_\theta}{\partial \theta}\right)+v_z\left(\frac{\partial v_\theta}{\partial z}\right)+\frac{v_r v_\theta}{r}\right)$$
$$=-\frac{1}{r}\left(\frac{\partial p(r,z)}{\partial \theta}\right)+\rho g_\theta+\mu\left(\frac{\partial}{\partial r}\left(\frac{1}{r}\frac{\partial(r v_\theta)}{\partial r}\right)+\frac{1}{r^2}\frac{\partial^2 v_\theta}{\partial \theta^2}+\frac{\partial^2 v_\theta}{\partial z^2}+\frac{2}{r^2}\left(\frac{\partial v_r}{\partial \theta}\right)\right)$$

z – component

$$\rho\left(\frac{\partial v_z}{\partial t}+v_r\left(\frac{\partial v_z}{\partial r}\right)+\frac{v_\theta}{r}\left(\frac{\partial v_z}{\partial \theta}\right)+v_z\left(\frac{\partial v_z}{\partial z}\right)\right)$$
$$=-\left(\frac{\partial p(r,z)}{\partial z}\right)+\rho g_z+\mu\left(\frac{1}{r}\frac{\partial}{\partial r}\left(r\frac{\partial v_z}{\partial r}\right)+\frac{1}{r^2}\frac{\partial^2 v_z}{\partial \theta^2}+\frac{\partial^2 v_z}{\partial z^2}\right)$$

Navier-Stokes Equations for 1- D Model

- **r – component**

$$-\frac{\rho v_\theta{}^2}{r} = -\left(\frac{\partial p}{\partial r}\right)$$

- **θ – component**

$$0 = -\left(\frac{d}{dr}\left(\frac{1}{r}\frac{d}{dr}(r v_\theta)\right)\right)$$

- **z - component**

$$0 = -\frac{\partial p}{\partial z} - \rho g_z$$

➢ **Outer Cylinder is Rotating**

- $$T_z = (-\tau_{r\theta})\Big|_{r\,=\,\kappa R}(2\pi\kappa R L)(\kappa R)$$

$$= 4\pi\mu\Omega_0 R^2 L\left(\frac{\kappa^2}{1-\kappa^2}\right)$$

➢ **Inner Cylinder is Rotating**

- $$T_z = (-\tau_{r\theta})\Big|_{r\,=\,R}(2\pi R L)(R)$$

$$= 4\pi\mu\Omega_i R^2 L\left(\frac{\kappa^2}{1-\kappa^2}\right)$$

⟵ **Torque Equation**

➢ **Outer Cylinder is Rotating and Inner Cylinder is Stationary**

B.C. 1 at r = κR, $\nu_\theta = 0$

B.C. 2 at r = R, $\nu_\theta = \Omega_o R$

$$\nu_\theta(r) = \Omega_0 R\left(\frac{\left(\frac{r}{\kappa R} - \frac{\kappa R}{r}\right)}{\left(\frac{1}{\kappa} - \kappa\right)}\right)$$

➢ **Inner Cylinder is Rotating and Outer Cylinder is Stationary**

B.C. 1 at r = κR, $\nu_\theta = \Omega_i R$

B.C. 2 at r = R, $\nu_\theta = 0$

$$\nu_\theta(r) = \Omega_i \kappa R\left(\frac{\left(\frac{R}{r} - \frac{r}{R}\right)}{\left(\frac{1}{\kappa} - \kappa\right)}\right)$$

Computing on CFD Module in COMSOL

Meshed Geometry

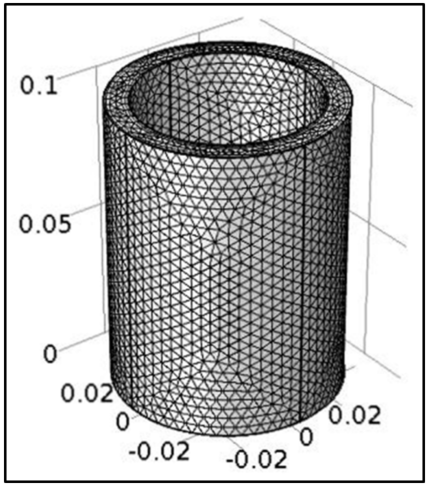

The 3-D geometry of concentric rotating cylinder system where the inner cylinder is rotating and outer cylinder is stationary was developed by using the *COMSOL Computational Fluid Dynamics* (CFD) module for determination of the velocity and pressure profiles.

3D meshing element type

Nodes: Cylinder

Boolean & Partitions

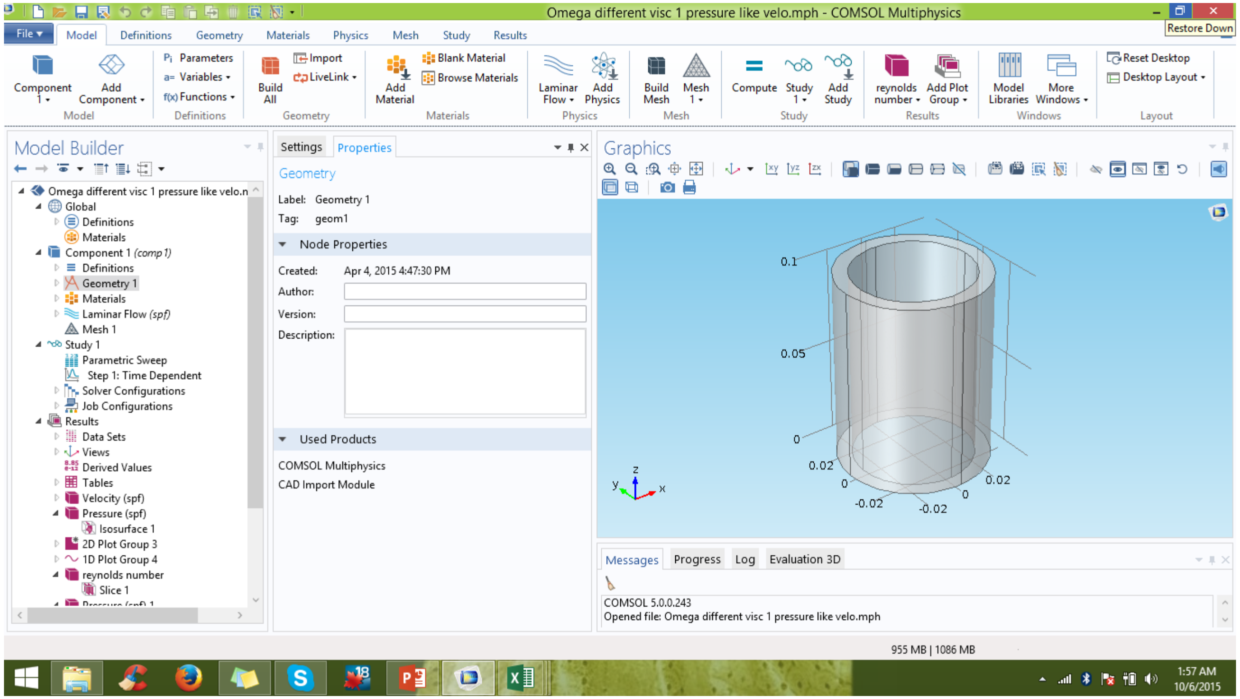

1–D Model

Velocity Profiles in the Annulus at Various Rotational Speeds

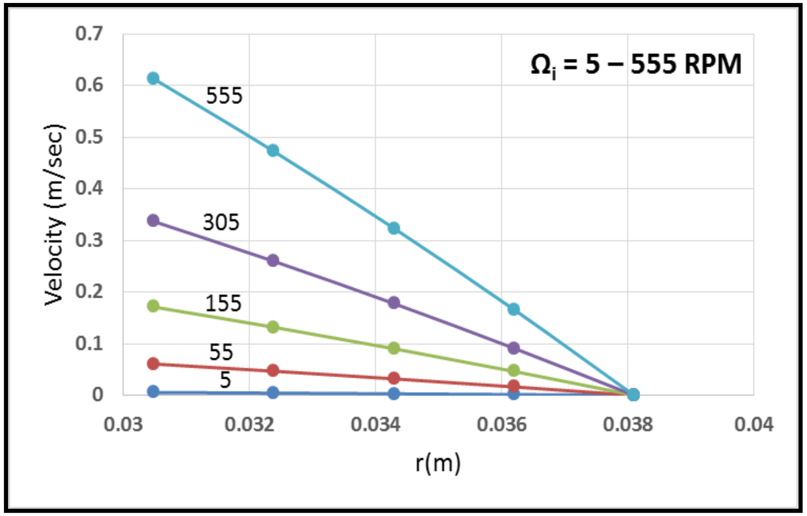

When inner cylinder is rotating

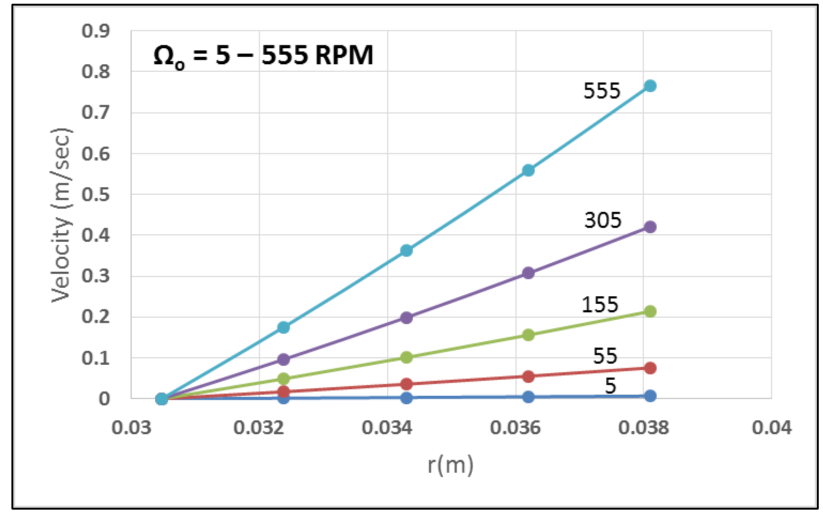

When outer cylinder is rotating

Torque Profile at Various Rotational Speeds

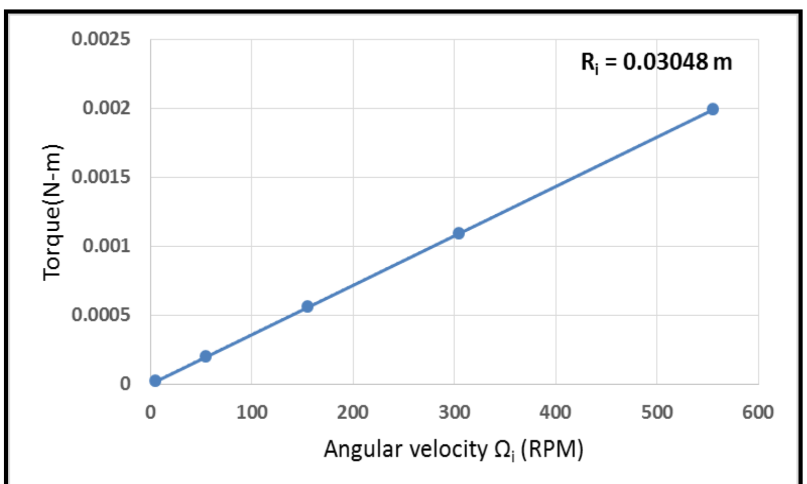

Reynolds Number Distribution Profile

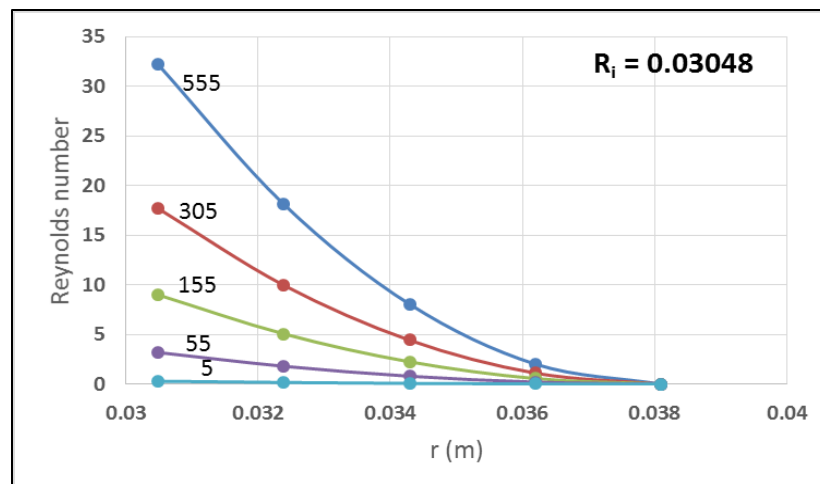

3 – D Model Images from COMSOL

Effect of Cylinder Inner Radius on Fluid Velocity Profiles

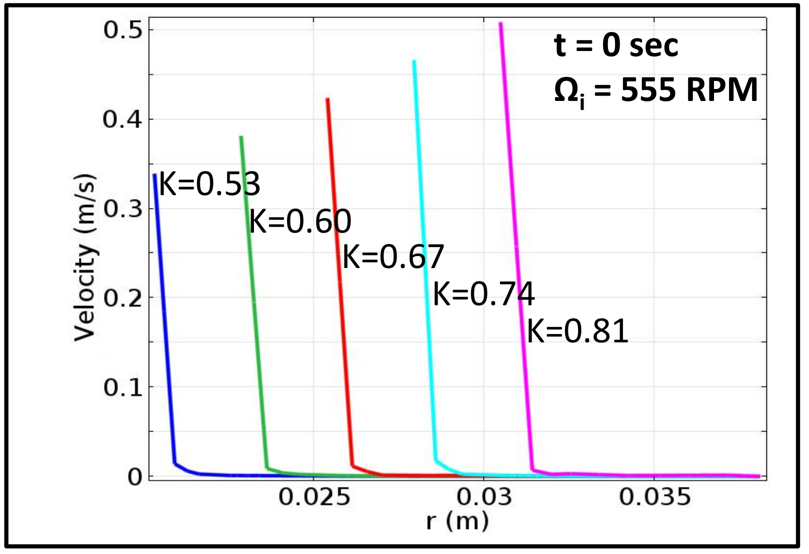

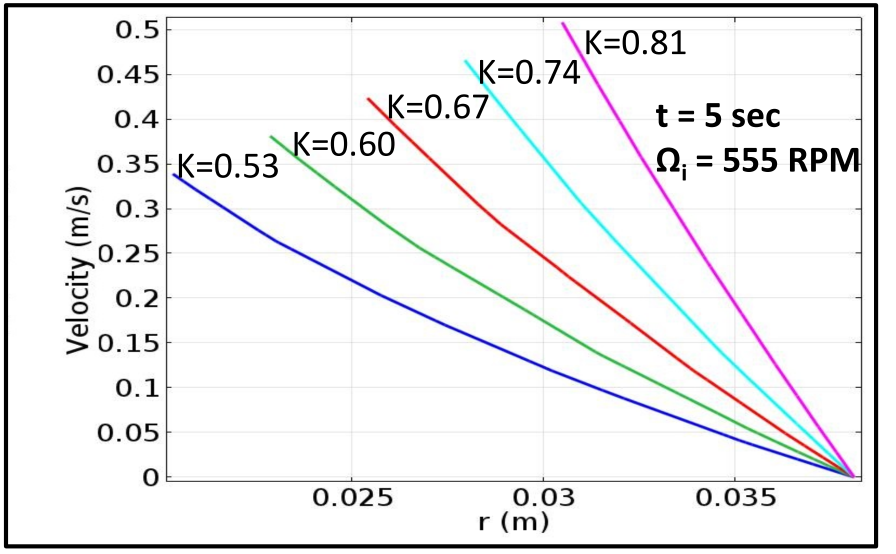

Developing Velocity Profiles During Cylinder Startup

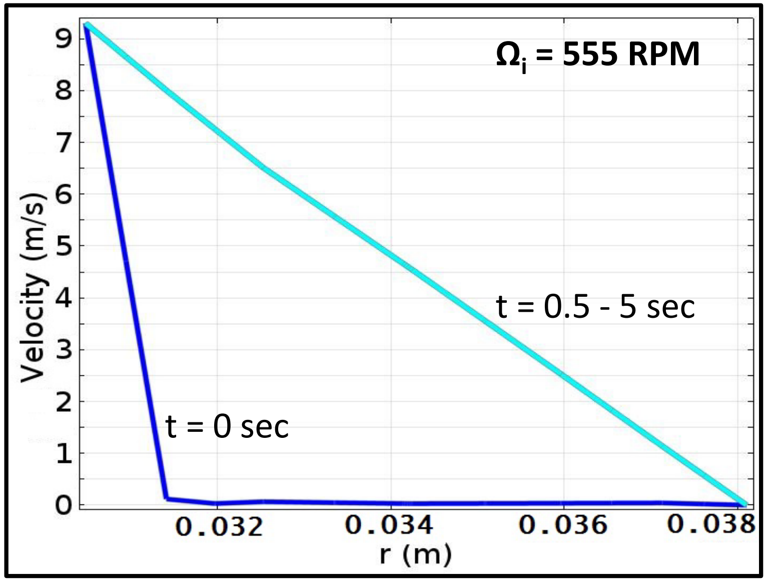

Velocity Profiles in the Annulus at Various Rotational Speeds

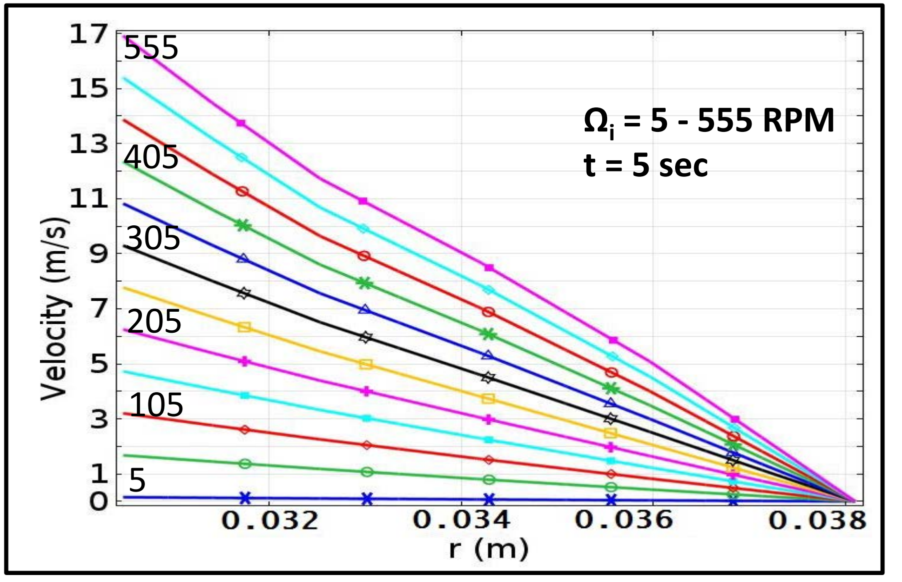

Velocity Profiles for 3–D Model

Rotating Inner Cylinder and Stationary Outer Cylinder

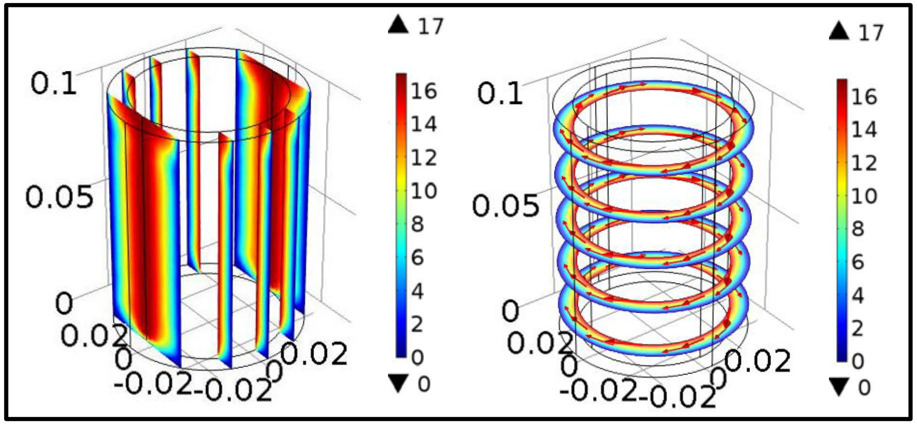

Velocity profiles at t = 5 sec and Ω_i = 555 RPM

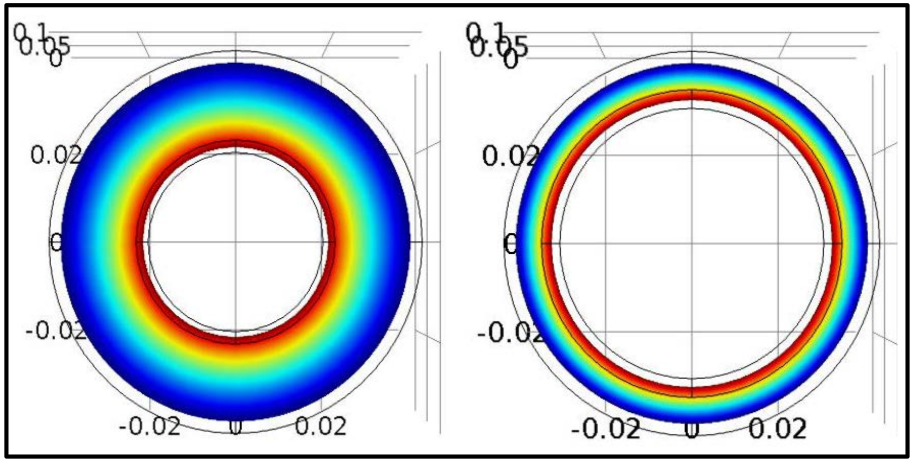

Velocity profiles when R_i is varied

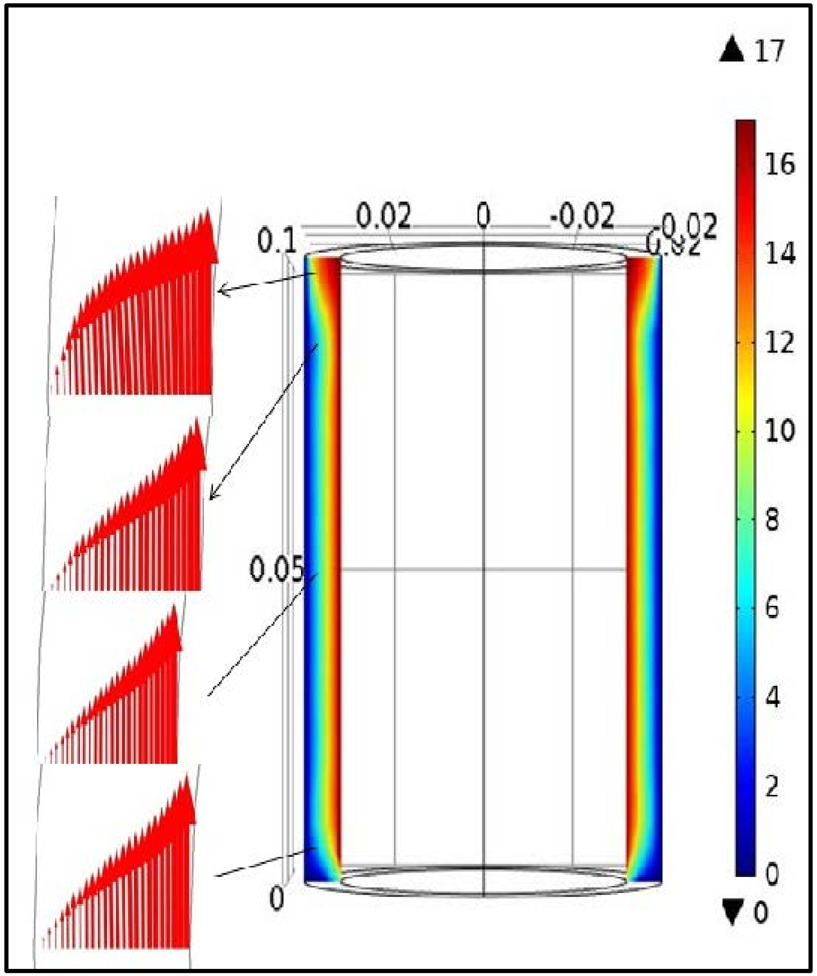

Velocity profile along the length of the cylinder

Profiles for 3–D Model in Different planes

Shear rate profiles at t = 5 sec and Ω_i = 555 RPM

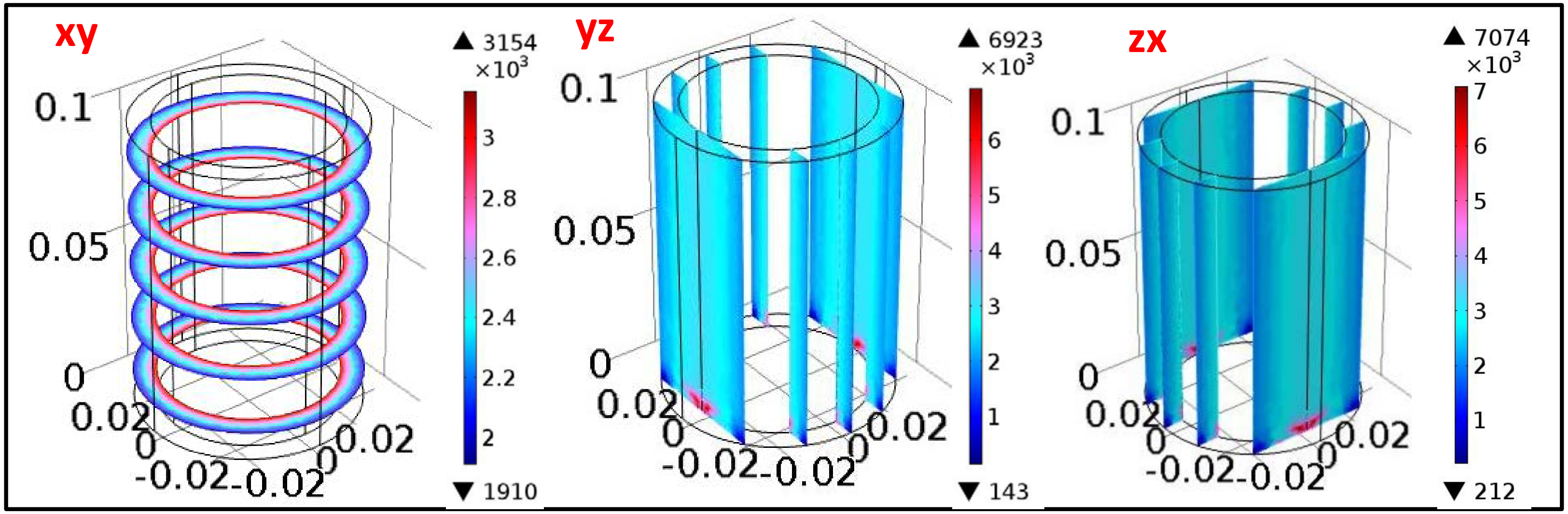

Shear stress profiles at t = 5 sec and Ω_i = 555 RPM

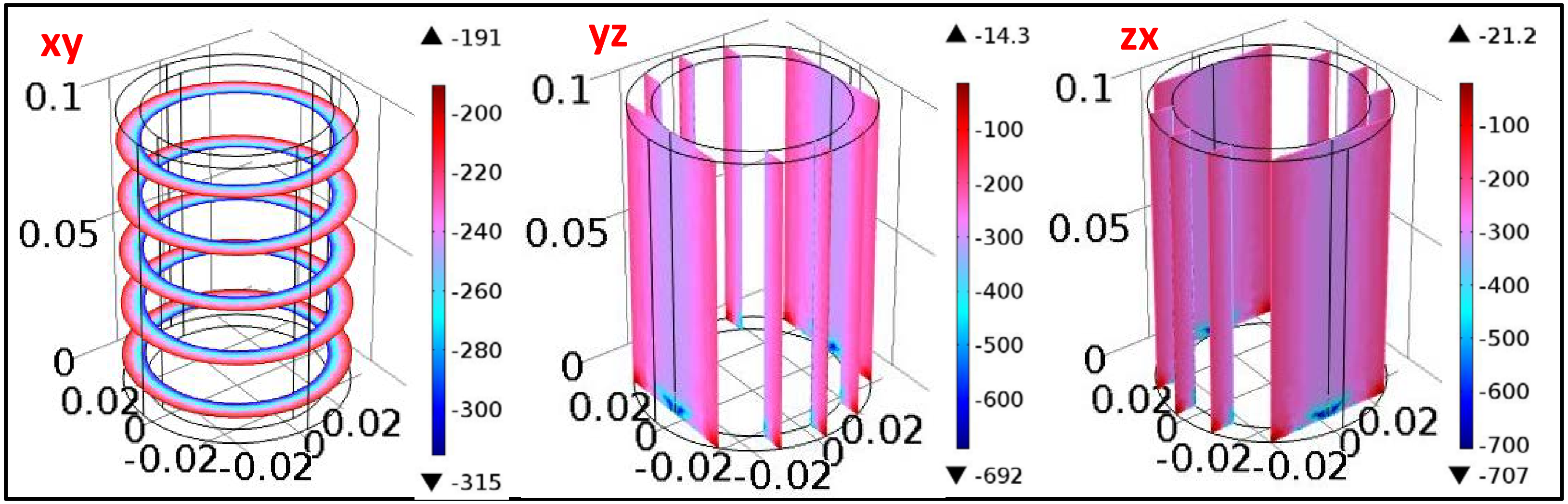

Profiles for 3–D Model in Different planes

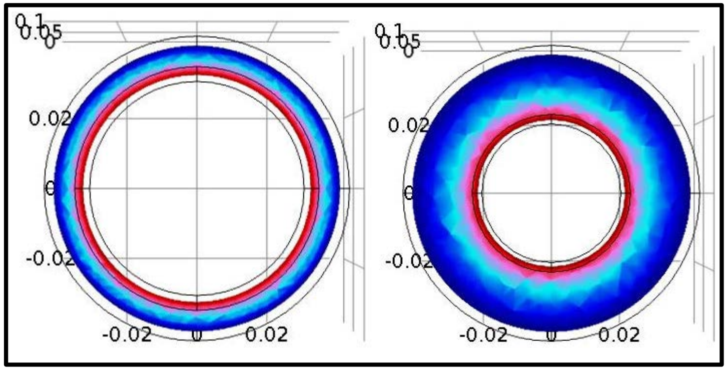

Shear rate profiles when R_i is varied

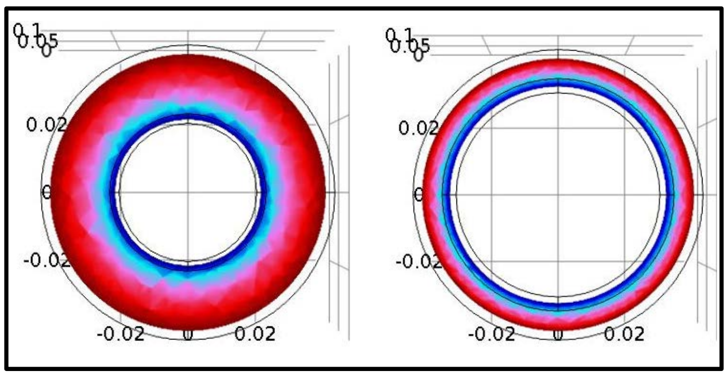

Shear stress profiles when R_i is varied

Shear stress profile versus length of the cylinder

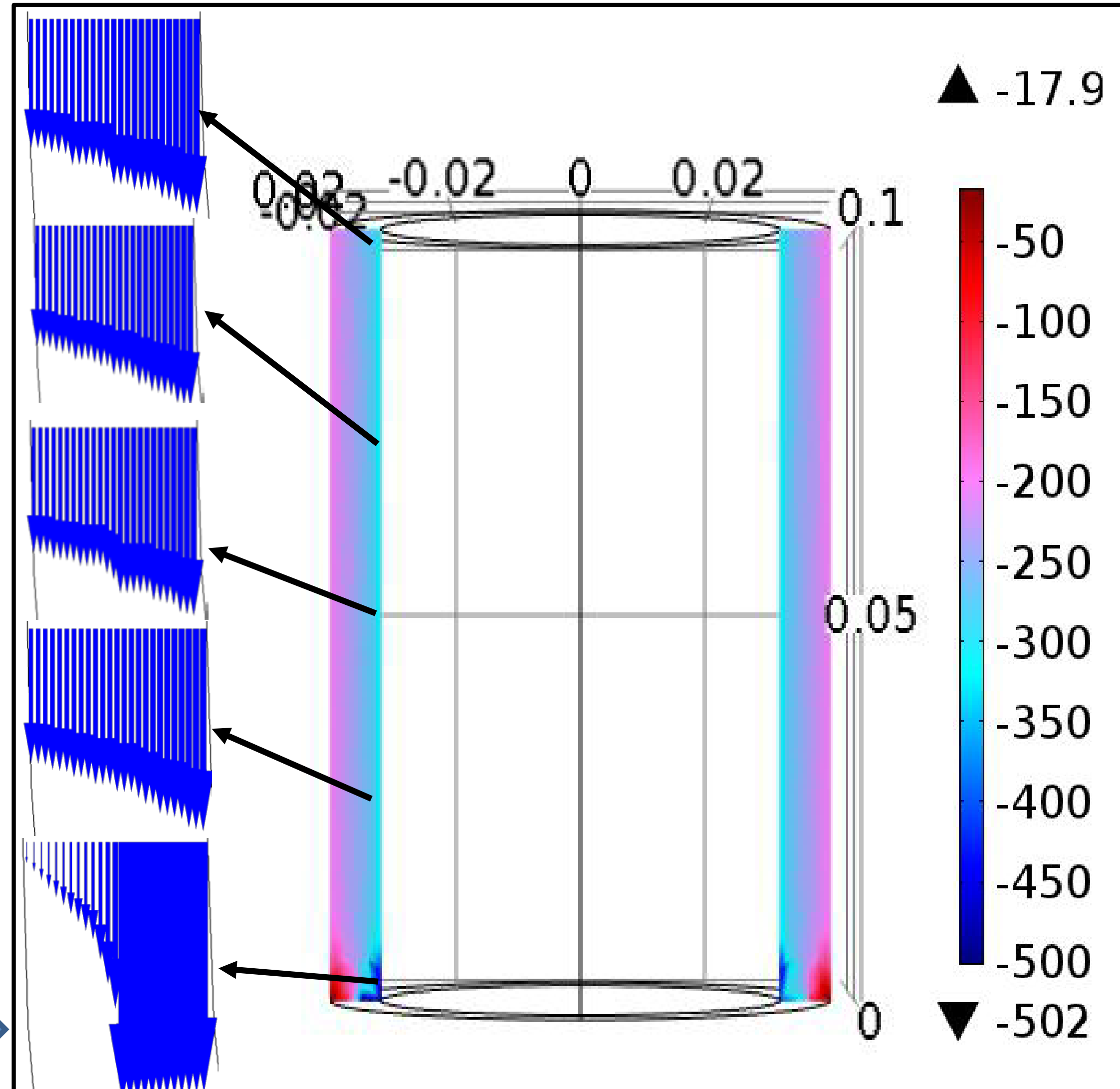

Pressure Profiles for 3–D and 1-D Model

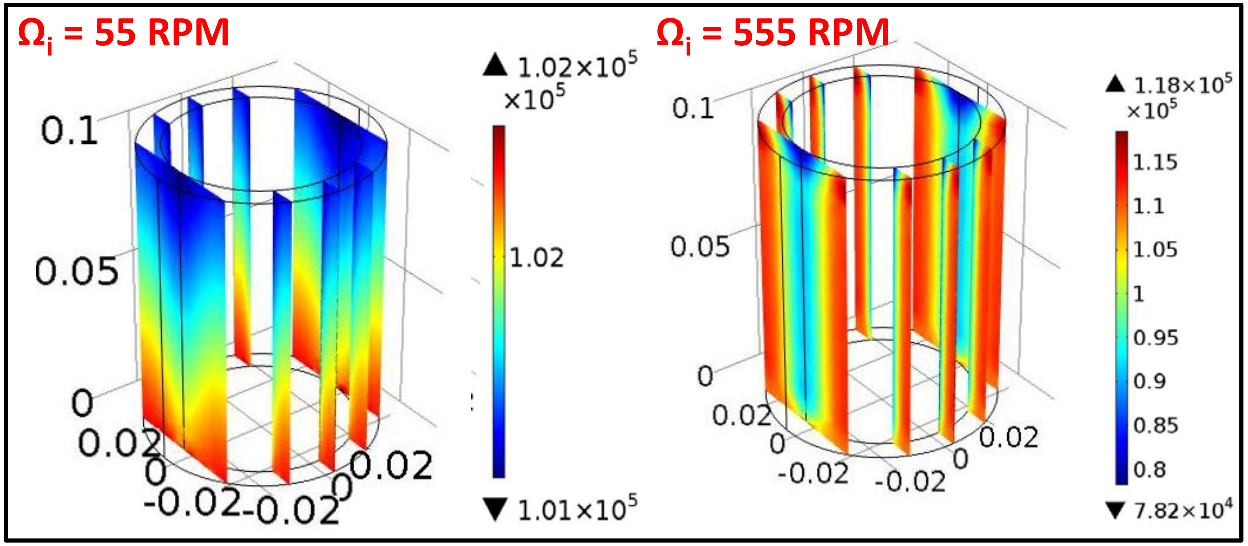

3-D Pressure profiles at t= 5 sec

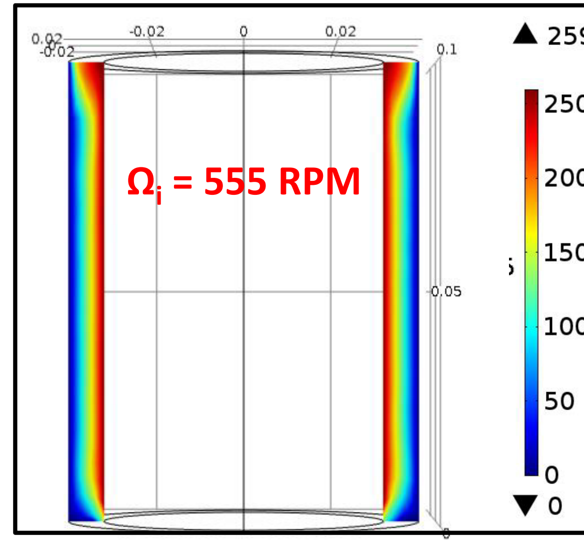

Reynolds number distribution

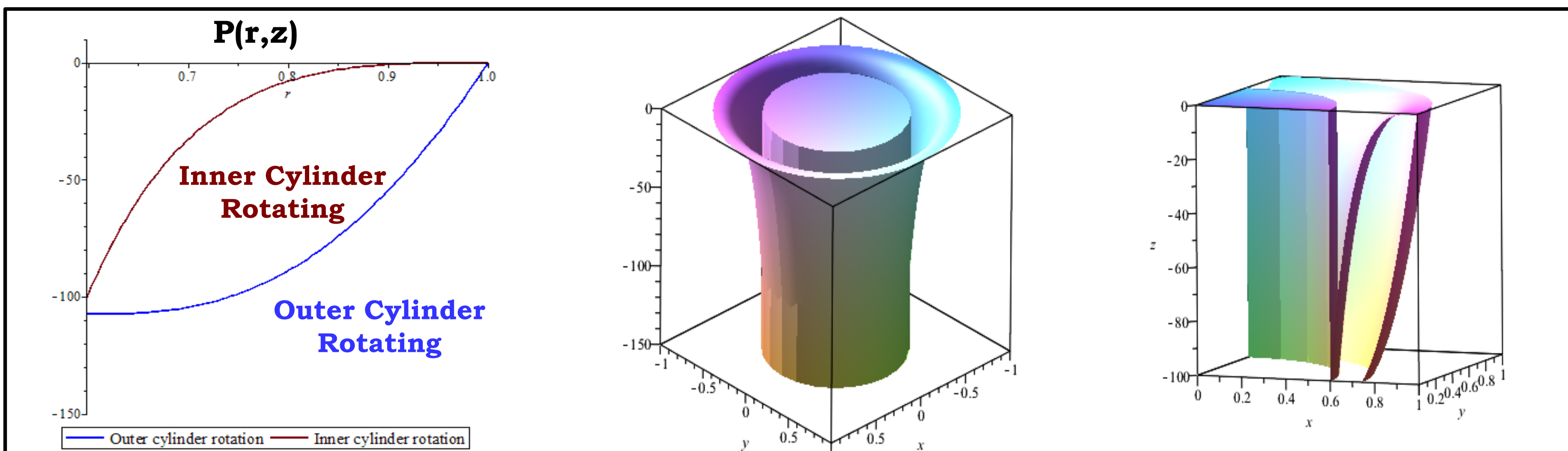

1-D Pressure profiles at t= 5 sec 555 RPM

Computational Challenges

When we try to run the system for turbulent flow, it became difficult to converge the model and if it converge for lower values of rotational speeds, we were unable to get stable results.

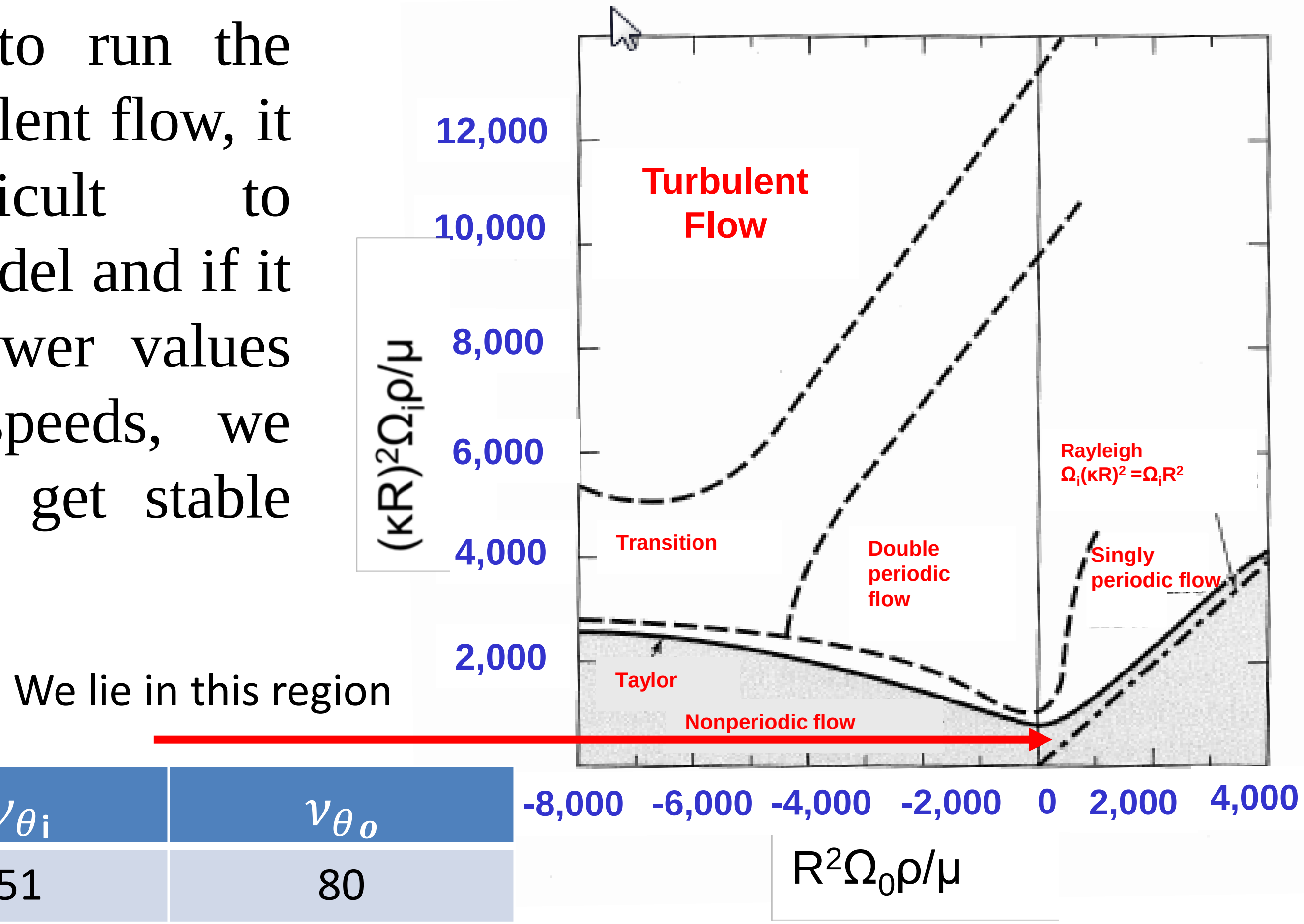

Omega	$\nu_{\theta i}$	$\nu_{\theta o}$
55	51	80
555	516	806

$\nu_{\theta i}$ = When Inner Cylinder is rotating and Outer Cylinder is Stationary

$\nu_{\theta 0}$= When Outer Cylinder is rotating and Inner Cylinder is Stationary

Key Observations

- The velocity profile approaches a becomes fully developed state only after traveling a distance that is several times the annular gap width.
- The analytical solution for the case where the fluid velocity profile depends only on the azimuthal component of the velocity vector in the radial direction is compared to the 3-D solution and shown to have good agreement in the fully-developed zone.
- The pressure gradient increases with increasing rotational speed.
- The value of shear stress acting on inner rotating cylinder is minimum and it is at it's maximum on the outer stationary wall.
- By this study a foundation has been laid for further application to non-Newtonian fluids used in drilling muds or separation.